Lithuanian Journal of Physics, Vol. **46**, No. 3, pp. 311–319 (2006)

EFFECT OF ANNEALING ON OPTICAL PROPERTIES OF InGaN / GaN MULTIPLE QUANTUM WELLS

Y.-C. Cheng [a], S.-W. Feng [a], C.C. Yang [a], C.-T. Kuo [b], J.-S. Tsang [b], S. Juršėnas [c], S. Miasojedovas [c], and A. Žukauskas [c]

[a] *Graduate Institute of Electro-Optical Engineering and Department of Electrical Engineering, National Taiwan University 1, Roosevelt Road, Sec. 4, Taipei, Taiwan, R.O.C.*

[b] *Advanced Epitaxy Technology Inc., Hsinchu Industrial Park, Hsinchu, Taiwan, R.O.C.*

[c] *Institute of Materials Science and Applied Research, Vilnius University, Saulėtekio 9, LT-10222 Vilnius, Lithuania*

E-mail: saulius.jursenas@ff.vu.lt

Received 24 February 2006

Site-selective photoluminescence, photoluminescence excitation, and time-resolved luminescence in as-grown and thermally treated $In_{0.15}Ga_{0.85}N$ / GaN multiple quantum wells (MQWs) was investigated as a function of well width in the temperature range of 10–300 K. Thermal annealing at 800 °C for 30 min monitored by microstructure imaging was shown to result in an alteration of MQWs optical properties intricately depending on the well thickness. The observed blue shift of the luminescence band and pronounced changes in the absorbance indicate a remarkable interdiffusion of indium at the quantum well–barrier interface for MQWs with thin (2 nm) wells. Meanwhile for thicker (3 nm) wells, a pronounced red shift of the luminescence band and an increase in the luminescence decay time was observed and attributed to electron–hole wave function separation facilitated by the smoothened band potential profile. In the thickest wells (4 nm), annealing resulted in even more pronounced improvement of microstructure, which led to a noticeable reduction of the localization energy of the electronic excitations (an annealing-invoked luminescence peak blue shift that overweighs the red one caused by intrinsic field) and to suppression of nonradiative recombination (an increase in luminescence efficiency). The results are accounted for in terms of annealing-invoked In–Ga interdiffusion, which behaves as either diffusion of indium to barriers or "uphill" diffusion within the wells depending on the well width.

Keywords: InGaN, multiple quantum wells, annealing, luminescence

PACS: 78.55.Cr, 78.47.+p, 78.67.De

1. Introduction

InGaN-based multiple quantum wells (MQWs) are the key structures for manufacturing of violet, blue, and green light emitting diodes and laser diodes [1, 2]. Fabrication of the light emitting devices requires further optimization of the structures for increased efficiency and lifetime. Thermal treatment is one of the technological factors that may facilitate optimization of active, barrier, and contact layers. Typically during the epitaxial growth of InGaN / GaN structures and during the fabrication of devices, the structures undergo several high-temperature impacts [1]. However, thermal treatment introduced for a particular layer might have an unexpected impact on the other layers. In particular, thermal treatment can change the distribution of the indium composition and influence the strain in the quantum wells through ordinary diffusion [3–5] and "uphill" (strain-induced) diffusion [6–9].

Usually thermal annealing is related to indium and gallium interdiffusion across the interface of quantum-well and barrier layers [3–5]. This results in a blue shift of the photoluminescence (PL) and absorbance spectra [5]. A complete merging of the barrier and well layers has been observed in an InGaN / GaN structure after annealing at high temperature [4]. On the other hand, In–Ga interdiffusion in InGaN alloys is rather intricate because of immiscibility of InN and GaN materials, which can result in phase separation in InGaN layers [6, 7]. Since InGaN alloys usually are grown at temperatures below 1473 K, the critical temperature above which the InN–GaN system is completely miscible [10, 11], in all InGaN alloys the phase separation is expected based on thermodynamics considerations. The phenomenon of InGaN phase

© Lithuanian Physical Society, 2006
© Lithuanian Academy of Sciences, 2006

ISSN 1648-8504

separation [6–14] is of considerable interest, since InN-rich regions were reported to play a crucial role in light generation in nitride-based light emitting structures [15–19]. Phase separation has been observed using several growth techniques, preferably in thick films [6–9, 12].The observed phase separation is evidently driven by strain due to the mixing of the two lattice mismatched components of the InGaN alloy system. Indium atoms are expelled from the InGaN lattice that results in an occurrence of an alloy of different composition and in a reduced strain energy of the system. It has been predicted that for a standard growth temperature, spinodal decomposition occurs for indium concentration above 20% [10, 11]. Post-growth thermal annealing was reported to facilitate the formation of indium-rich regions in InGaN quantum wells [6–9, 13]. On the other hand, thermal annealing can lead to redistribution of strain energy and reduced phase separation, which is sensitive to strain effects. Both phase separation and strain effects are expected to enhance with increasing the InGaN well width. Therefore, the annealing-induced In diffusion mechanism can be dependent on well width.

In the present work, the impact of post-growth thermal treatment on optical properties of InGaN / GaN MQWs with various well layer thicknesses was investigated. As-grown and annealed samples, which display different images of high-resolution transmittance electron microscopy (HRTEM), were investigated by site-selective PL observation-energy-selective photoluminescence excitation (PLE), temperature dependent PL, and time-resolved photoluminescence (TRPL). Distinct changes of the MQWs optical properties for the samples of different well layer thickness were linked with the microstructure changes invoked by thermal treatment.

2. Experimental details

The samples were grown on c-plane sapphire by metalorganic chemical vapour deposition. Following the deposition of 30 nm GaN buffer layer and a 2.3 μm GaN layer, MQW structures consisting of five pairs of $In_{0.15}Ga_{0.85}N$ well and 10 nm thick GaN barrier were grown. Three samples with different well widths of 2, 3, and 4 nm were prepared and referred to as samples *w20*, *w30*, and *w40*, respectively. The growth temperatures were 1010 and 720 °C for GaN and InGaN, respectively. A set of three as-grown samples and three counterpart ones thermally annealed in a quartz tube furnace at 800 °C in nitrogen ambient for 30 min was investigated.

A continuous wave He–Cd laser (photon energy $h\nu = 3.812$ eV) was used for PL excitation. The samples were placed in a cryostat for temperature dependent measurements. For TRPL measurements, a Verdi^{TM} laser-pumped mode-locked Ti : sapphire laser with 100 fs pulse width and with frequency doubling by a beta barium borate (BBO) crystal was used ($h\nu = 3.177$ eV). Luminescence from the sample was collected and focused into a spectrometer prior to imaging in a Hamamatsu streak camera. The temporal resolution of the operation mode was 4.7 ps. PLE experiments were conducted using quasi-monochromatic excitation light source from a xenon lamp dispersed by a 0.15 m monochromator. The bandwidth of the excitation light from the xenon lamp was set at less than 3 nm.

HRTEM investigations were carried out by a 200 keV Philips CM 200 and a 300 keV JEM 3010 microscopes. All the high-resolution micrographs were taken at Scherzer defocus and the sample was viewed along a [11$\bar{2}$0] zone axis. The 300 keV JEM 3010 microscope was equipped with a 2000$\times$2000 slow-scan CCD camera and a Gatan Imaging Filter. HRTEM pictures are exposed for a reasonably short period of time in order to reduce alteration of the specimen [20, 21]. The main reasoning is based on comparison of the images of as-grown and annealed samples.

3. Results

3.1. High-resolution transmission electron microscopy of InGaN / GaN MQWs

Figure 1 shows the HRTEM images of the as-grown (a–c) and annealed (d–f) samples of various well thickness, respectively. The periodic structure of MQWs can be clearly resolved in all images. Darker areas in the images correspond to the regions of an increased indium concentration and / or enhanced strain.

Typically for ternary InGaN system, the In concentration and strain are rather randomly distributed along MQW layers. Although all our as-grown samples nominally contain the same molar fraction of indium, actual phase separation pattern in the layers of various thickness might be different. Growth of MQWs of a lager thickness requires longer time, thus the quantum well layers have more time for strain relaxation and phase separation. Eventually, more pronounced fluctuations

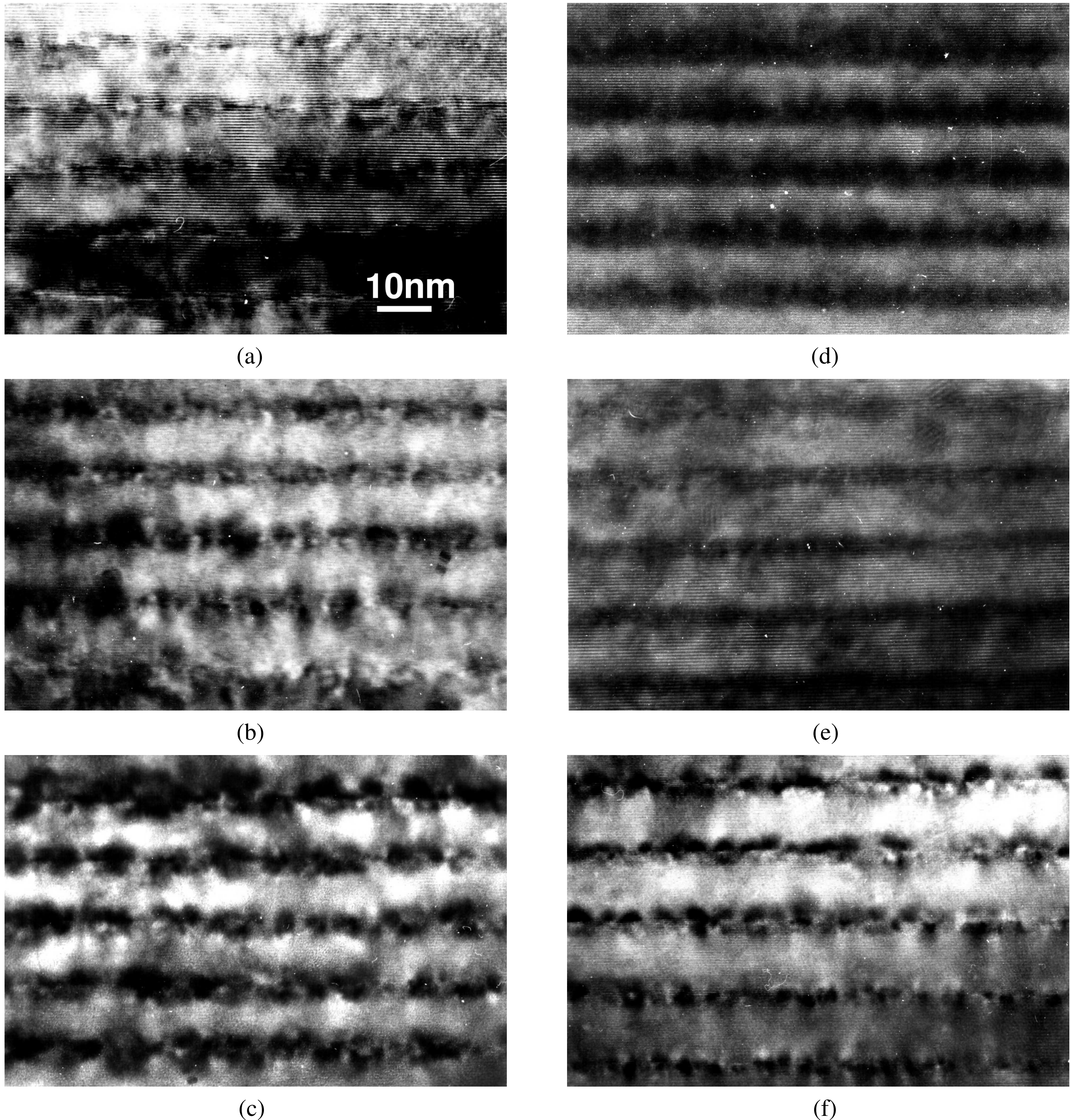

Fig. 1. HRTEM images of the as-grown (a) *w20*, (b) *w30*, (c) *w40* and annealed (d) *w20*, (e) *w30*, (f) *w40* samples.

of indium content are expected. This can result in different impact of thermal annealing. The *w20* as-grown sample (Fig. 1(a)) exhibits rather diffusive distribution of strain and indium content, although distinct positions of QWs can be identified. After thermal annealing, the dark areas in the images related to the QWs enhance and occupy a remarkable part of the barrier region (Fig. 1(d)). This allows us to make a suggestion about indium interdiffusion in to the barriers and / or enhancement of strained interface regions due to thermal annealing in thin *w20* layers.

The thicker MQWs *w30* (Fig. 1(b, e)) and *w40* (Fig. 1(c, f)) show opposite structural changes under thermal treatment. After thermal treatment, initially large and randomly distributed around QWs dark regions become thinner. This suggests "uphill" diffusion of indium and / or reduction of strain in the interface regions of thick InGaN / GaN MQWs.

To verify the suggestions that follow from the

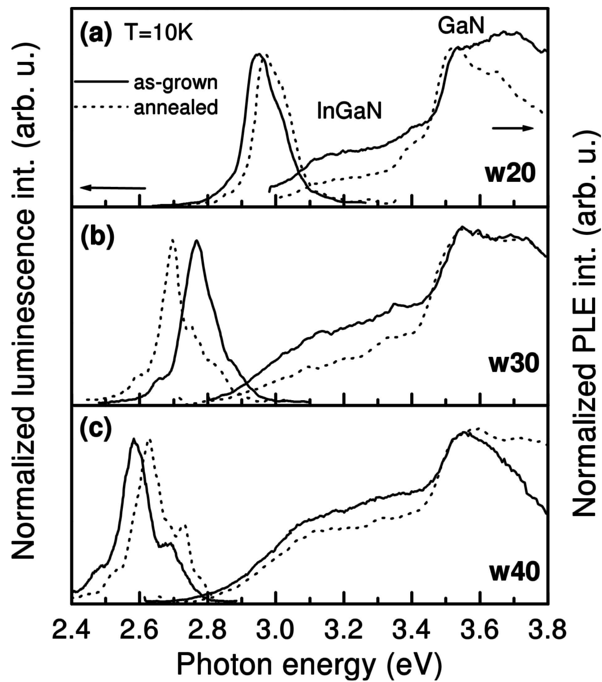

Fig. 2. Normalized photoluminescence spectra and photoluminescence excitation spectra of as-grown (solid line) and annealed (dotted line) InGaN / GaN MQWs (a) *w20*, (b) *w30*, and (c) *w40*, measured at 10 K.

analysis of microstructure revealed by HRTEM images, the impact of thermal treatment on optical properties of the MQWs is considered in detail below.

3.2. Low-temperature site-selective PL and PLE spectroscopy

Solid lines on the left-hand side of Fig. 2 show normalized PL spectra of as-grown InGaN / GaN MQW samples obtained at 10 K. The main luminescence spectral properties are typical of low-temperature emission in InGaN / GaN MQWs [16, 18, 22]. The luminescence spectrum of the *w20* sample (Fig. 2(a)) consists of a main band at 2.958 eV, which can be attributed to localized exciton states, and its phonon replica located on the low energy wing at about 2.865 eV. The band at the high energy wing of the main luminescence band might be related to shallow impurity related centres [22]. The shape of the spectrum weakly depends on the excitation photon energy (not shown). Meanwhile, the luminescence intensity rapidly decreases with tuning of the excitation photon energy below 3.1 eV as it is seen in the PLE spectra. With increasing the well width of the as-grown samples, the luminescence spectra steadily redshifts with the main peak positioned at 2.767 eV and 2.589 eV for samples *w30* (Fig. 2(b)) and *w40* (Fig. 2(c)), respectively. The red shift is contributed by several impacts: (i) a decrease in quantum confinement energy, (ii) the quantum confined Stark effect (QCSE) due to an increase in electron–hole wave function separation caused by intrinsic field, and (iii) deeper localization of the electronic excitations due to an enhancement of disorder-related fluctuations of the band potential profile. At the same time, the bandwidth is seen to decrease with the well width: the estimated full with at half magnitude (FWHM) is 128, 108, and 89 meV for the samples *w20*, *w30*, and *w40*, respectively. The shape of the luminescence band becomes more sensitive to the excitation photon energy with increasing the well width (not shown): the band broadens and blueshifts with an increase of the excitation photon energy. This can be attributed to an enhancement of band potential fluctuations related to the growth time dependent phase separation on the growth surface [8, 9].

Solid lines on the right-hand side of Fig. 2 show PLE spectra of the *w20*, *w30*, and *w40* as-grown samples. The PLE spectra exhibit typical dependences of MQW structures with spectral variation in optical density of the QW (InGaN) and barrier (GaN) materials reflected. The PLE signal is much stronger for the excitation photon energy above 3.5 eV due to the larger thickness of the barrier layer (10 nm). The boundary between the PLE features of InGaN and GaN layers is sharp due to the edge of excitonic absorbance in GaN. The absorbance edge of InGaN material below 3.1 eV is less steep indicating on the presence of compositional fluctuations, which were seen in the HRTEM images.

With an increase in well width from 2 to 4 nm, pronounced changes can be revealed in the well absorbance region: (i) an increase in PLE signal due to increased optical density of the InGaN layer, (ii) a redshift of about 66 meV that is in line with the quantum confinement effect (note, that intrinsic electric field can also affect excitonic absorbance spectrum), (iii) a pronounced sensitivity of the PLE signal intensity to the observation photon energy (not shown). The latter effect is due to aforementioned sensitivity of the shape of the luminescence band to the excitation photon energy in thicker wells, which is an indication of increased disorder.

In addition, a pronounced difference in the PLE signal caused by absorbance in the GaN barrier layers ($h\nu > 3.50$ eV) is peculiar for different well widths. Instead of a rising dependence, which is predictable for a MQW structure of good quality, a significant decline of the PLE signal for the excitation photon energy above 3.50 eV is observed in the as-grown structures with increased well width. This can be attributed to an

enhancement of nonradiative capture of just photogenerated excitons (electrons and holes) with a higher initial excess energy. To produce luminescence from the QW states, the excitons (carriers) excited in the barrier layer are to be captured in the well. However, excitations with a larger excess energy have a smaller well-capture probability and, consequently, a higher overall probability of trapping to nonradiative centres. Thus, the decline in the PLE spectra for $h\nu > 3.50$ eV can be explained under assumption that increased well width results not only in reduced quality of the well material but also of the barrier and / or interface. This is in line with the HRTEM images (Fig. 1(a–c)) where an increased patterning of the barrier layers in the as-grown samples with increased well width can be distinguished.

Dotted lines in Fig. 2 show normalized PL and PLE spectra of annealed InGaN / GaN MQWs measured at 10 K. The PL spectrum of the annealed *w20* sample blueshifts by about 20 meV in comparison with the as-grown one (Fig. 2(a)). The PL spectrum of the annealed *w30* sample redshifts by about 71 meV, while that of the *w40* sample blueshifts by about 45 meV. This indicates an intricate impact of thermal treatment on the luminescence properties of MQWs of various well widths.

The PLE spectra (dotted lines on the right-hand side of Fig. 2) show significant spectral changes as well. (The spectra are normalized at 3.50 eV to reveal spectral changes occurring upon annealing.) The most pronounced impact of thermal treatment appears for the thin-well sample *w20* (Fig. 2(a)). A decline of the spectral dependence of the PLE signal in the barrier spectral region at $h\nu > 3.50$ eV evidences a remarkable increase in nonradiative trap density. This is in line with significant reduction of the luminescence efficiency (see below). Additionally, by detailed comparison of the spectra a blue shift of the PLE feature due to wells at the absorbance edge can be distinguished concurrently with the blue shift of the PL line. These observations support a suggestion drawn from the microstructure analysis that thermal treatment results in In interdiffusion from the well layers to the barriers [3–5].

The impact of thermal treatment on the PLE spectra of the thicker QW layers is of opposite character (Fig. 2(b, c)). The sample *w30* shows little changes in the PLE spectrum in the barrier spectral region $h\nu > 3.50$ eV, while the even thicker *w40* sample shows an opposite trend: thermal treatment results in a flatter spectral dependence indicating on reduction of the nonradiative traps. Again, this is in line with the narrowing

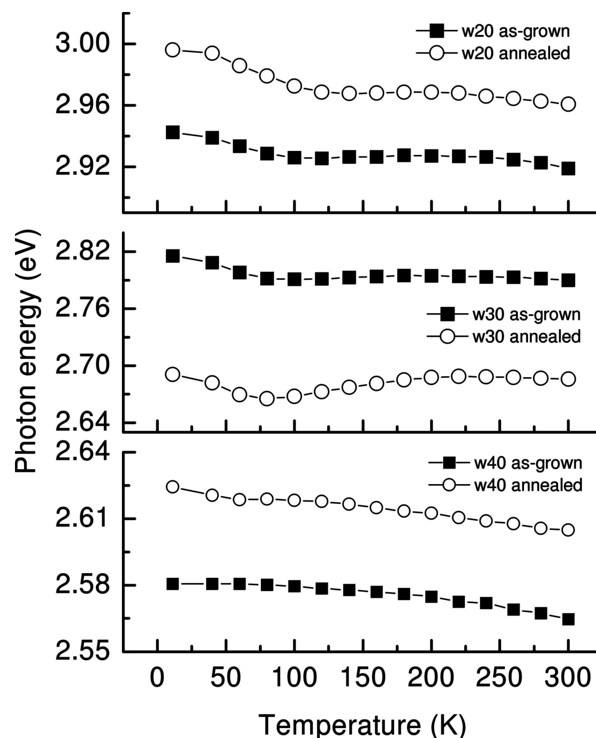

Fig. 3. Variations of PL peak positions versus temperature of as-grown and annealed samples (a) *w20*, (b) *w30*, and (c) *w40*.

of the dark regions in the HRTM images (Fig. 1(c, f)). The QW absorbance edge becomes flatter for the *w30* sample and steeper for the *w40* sample. As discussed below, such behaviour might be due to several impacts such as indium diffusion, increase in disorder due to composition fluctuations, and electron–hole wave function separation due to intrinsic field.

3.3. Temperature dependent PL and TRPL

The temperature variations of the PL peak position in the three pairs of the as-grown and annealed samples are shown in Fig. 3. Both before and after thermal annealing, the characteristic "S" shape variation of the PL peak can be distinguished in each case indicating on migration of excitations within spectrally and spatially disordered system [23, 24]. In both the as-grown and annealed samples, the amplitude of the initial decrease in peak energy diminishes with the well thickness. As revealed by Monte Carlo simulation of exciton hopping [23, 24], this can be attributed to an increase in spatial separation between the localized states in thicker wells that is in line with enhanced In segregation seen in HRTEM images (Fig. 1). Similar behaviour might be caused by reduced lifetime of the excitons or carriers; however, our TRPL results indicate that lifetime increases with the well width. This increase in carrier lifetime is typical for spatial separation of electron and

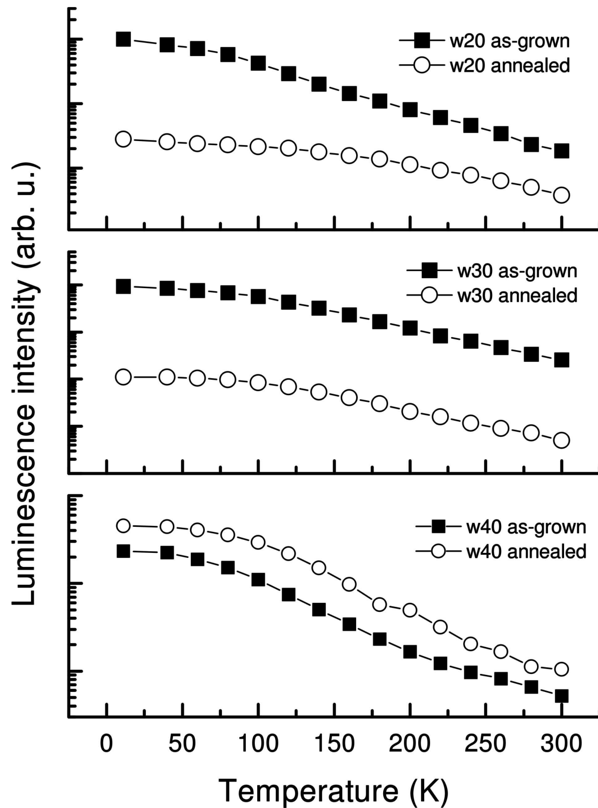

Fig. 4. Variations of PL intensities versus temperature of as-grown and annealed samples (a) *w20*, (b) *w30*, and (c) *w40*.

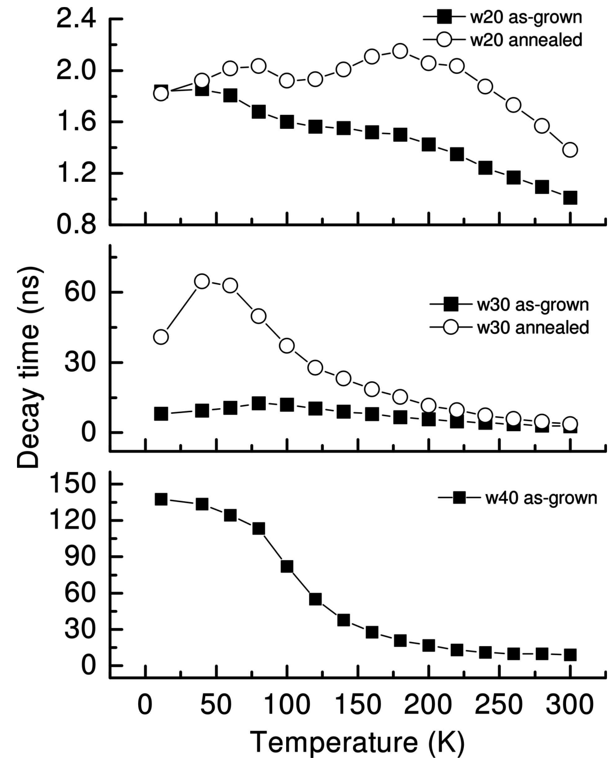

Fig. 5. Variations of PL decay times versus temperature of as-grown and annealed samples (a) *w20*, (b) *w30*. That of the as-grown *w40* is also shown.

hole wave functions in thicker wells (QCSE). It should be noted that temporal profile of MQWs luminescence with partially screened intrinsic field generally is non-exponential and here, for simplicity, averaged values of luminescence decay time were used. The "S" shape becomes more pronounced in the annealed samples. Again, this can be attributed to a decreased spatial separation between the localized states and / or increased lifetime. To our opinion in the thin wells (*w20*), the major effect is due to increased lifetime (see Fig. 5(a)), whereas in the thicker wells (*w30* and *w40*) both effects might be important.

Figure 4 shows temperature dependent variations of the integrated PL intensity in the as-grown and annealed samples. Thermal treatment is seen to cause a significant reduction in PL intensity in the *w20* sample (Fig. 4(a)), in agreement with the suggestion on In interdiffusion and consequent degradation of the barriers and interfaces. Correspondingly, the flatter temperature dependence in the annealed sample is an indication of a larger energy required for delocalization, which facilitates nonradiative recombination [25]. Sample *w30* shows similar temperature dynamics (Fig. 4(b)), however without a remarkable change in the activation energy. This can be attributed to an increased role of electron–hole wave function separation due to intrinsic field in thicker wells that agrees with the observed red shift of the PL peak position (Fig. 2(b)). We suggest that such a separation is facilitated by a smoother potential profile in the annealed wells as evidenced by the HRTEM images and temperature dependence of the PL peak position. With further increase in well thickness (sample *w40*), the principal impact of annealing is an increase of the PL intensity in the entire range of temperatures. In combination with the blue shift of the PL peak position (Fig. 2(c)), such an increase can be attributed to a significant smoothing of the band potential profile and a subsequent decrease of the localization energy. An additional increase in PL intensity might be caused by a reduced number of nonradiative centres in the barrier layers and interfaces that is in agreement with the HRTEM images (Fig. 1(c, f)) and PLE spectra (Fig. 2(c)).

Figure 5 shows PL decay time at the PL spectral peaks as a function of temperature in the as-grown and annealed samples [14]. (In the annealed *w40* sample, the PL decay time becomes too long to be measured by our technique.) The low-temperature lifetime of the as-grown samples rapidly increases with the well width and is equal to 1.8, 9, and 137 ns for *w20*, *w30*, and *w40* samples, respectively. This increase is obviously due to

spatial separation of electron and hole wave functions in thicker wells [26, 27]. This is in line with the increase in Stokes shift with the well width (Fig. 2). Thermal annealing generally results in an increase of carrier lifetime, however, with the peculiarities dependent on the well width. In the *w20* sample, the lifetime alters negligibly at low temperature and exhibits a remarkable increase at elevated temperatures. This effect agrees with the temperature dynamics of the PL intensity in that annealing of a thin well results in an enhancement of potential fluctuations and in a higher energy required for delocalization, which initiates the nonradiative process [25]. Interestingly, despite the unchanged lifetime at low temperature, the annealed sample exhibits a lower PL efficiency (Fig. 4(a)), probably because of reduced rate of carrier capture to the well due to degraded barriers and / or interfaces. Contrarily, the thicker wells (*w30*) show a remarkable increase in low-temperature lifetime after thermal annealing, the difference between the as-grown and annealed samples disappearing with temperature (Fig. 4(b)). Such behaviour might be accounted for by an increased electron–hole wave function separation at low temperatures due to increased carrier / exciton diffusivity in the annealed sample. At elevated temperatures, annealing results in negligible changes of lifetime, since the excitations are delocalised. In the thickest sample (*w40*), localization energy is higher and annealing facilitates the QCSE in the entire temperature range.

4. Discussion

Our results on HRTEM, PL, PLE, and TRPL in InGaN / GaN MQWs revealed the dynamics of radiative and nonradiative processes being dependent on the well thickness and the impact of thermal treatment, which was shown to essentially depend on the quantum well width.

Quantum well width dependent dynamics of recombination processes in InGaN / GaN MQWs is usually explained by the QCSE and inhomogeneous distribution of indium as well as by nonradiative centres due to structural and point defects [15–17, 26–28]. Basically, dynamics of the QCSE with the well width is enough understood for a smooth band potential profile [26, 27]. Meanwhile, inhomogeneous distribution of indium, which results in fluctuations of the band potential profile, displays a much more intricate dependence on the well width. There are several studies on accumulation of indium atoms on the growth surface and generation of misfit dislocations with increasing the thickness of the InGaN layer [29, 30]. The concurrent plastic relaxation cannot be complete and homogeneous in all regions of the InGaN well, resulting in an inhomogeneous strain distribution within the layer. The inhomogeneous strain distribution could, in turn, enhance the local diffusion of indium atoms and thereby spinodally increases the composition fluctuations. Under favourable conditions, these fluctuations may result in phase separation [8, 9]. Phase separation requires long-range diffusion and a correlation should exist between phase separation and the growth time. The larger the layer thickness, the longer growth time is required, thus the quantum well layer has a longer time for strain relaxation and a more pronounced variation in indium content is expected. Our data on optical properties of InGaN / GaN MQWs allow one to infer that increasing the well width results in (i) increased potential profile fluctuations, which are known to remarkably influence the migration of electronic excitations, (ii) a modified nomenclature of nonradiative centres due to indium decomposition and modification of interfaces, (iii) enhanced spatial separation of the electron and hole wave functions in the wells.

Increased fluctuations of the band potential profile are evidenced by enhanced patterning of the HRTM images, by sensitivity of the PL spectra to the excitation photon energy, sensitivity of the PLE spectra to the observation photon energy, flattening of the well absorbance edge monitored by PLE, and smoothening of the "S"-shaped temperature dependence of PL with the increase in the well thickness. The decrease in carrier capture to the wells efficiency due to nonradiative recombination is clearly monitored by changes in the PLE spectrum in the barrier region. Enhanced spatial separation of the electron and hole wave functions is evidenced by a significant increase in carrier / exciton lifetime and by an increase in Stokes shift of PL, with both increases partially attributed to increased potential fluctuations. All these observations clearly indicate an increase in disorder with an increase of the well width.

Differences in degree of disorder of as-grown samples with various well widths lead to different impact of thermal annealing on luminescence from localized states. Since the average indium concentration in our samples is of 15%, only slightly below the critical value [10, 11], one can expect different trends in diffusion related processes (diffusion or spinodal decomposition) invoked by thermal treatment. Our data confirms that thermal annealing, which basically results in thermally activated In–Ga interdiffusion including "uphill" strain-induced diffusion and spinodal decomposition,

affects microstructure and strain in the wells, barriers, and interfaces. Eventually, thermal annealing modifies (i) the efficiency of carrier capture to the wells, (ii) electron–hole wave function separation within the wells, and (iii) nonradiative recombination rate, i. e. the basic processes, which govern the quantum efficiency of light generation in InGaN / GaN MQWs.

After thermal annealing, thinner samples that initially are of the best structural and optical quality are heavily deteriorated. We attribute this effect to indium interdiffusion into the barrier layers, which is monitored by the HRTM images. Annealing leads to changes in indium content as evidenced by the blueshift of the InGaN related emission and absorption bands. Indium interdiffusion also results in formation of a large amount of nonradiative defects both in the well and barrier that is confirmed by a significant reduction in luminescence efficiency and by modification of the PLE spectra in the barrier region. Meanwhile, no indications of changes in spatial separation of electrons and holes were distinguished, probably because of the well thickness being too small for the QCSE to manifest itself.

Thicker as-grown samples are already much more disordered due to indium segregation. This leads to an increase in the number of surface related defects. Increased thickness results in a noticeable enhancement of the QCSE that is monitored by the increased carrier lifetime, decreased PL efficiency, and red shift of the PL peak. Annealing seems to improve materials quality and to make potential profile smoother. The smoother potential profile facilitates electron–hole spatial separation, which results in the enhanced QCSE (an increase in the carrier / exciton lifetime, a decrease in PL efficiency, and the red shift of the PL band).

For the thickest samples investigated, thermal annealing results in even more significant improvement of microstructure that is evidenced by the narrowing of well-related dark regions in the HRTM images, as well as by modification of the barrier related PLE spectrum. This implies that indium is preferentially reorganized in the InGaN layers rather than diffused into GaN barriers. Consequent smoothening of the well potential profile leads to an increased electron–hole spatial separation due to intrinsic field. However the blue shift of the PL peak and an increase in PL efficiency show that annealing invokes a competing impact that outbalances the manifestation of the QCSE. We attribute this impact to improved microstructure, which results in shallower localization and remedy of nonradiative recombination centres.

5. Conclusions

Summarizing, temperature dependent site-selective PL, PLE, and TRPL study of three pairs of as-grown and annealed at 800 °C for 30 min $In_{0.15}Ga_{0.85}N$ / GaN MQWs with the well widths of 2, 3, and 4 nm were performed. Our results imply a nontrivial dependence of MQWs emission properties on thermal treatment. Differences in degree of disorder in as-grown samples of various well width leads to different impact of thermal annealing on luminescence from localized states. The blue shift of the PL peak and pronounced changes in the absorbance indicate a remarkable interdiffusion of indium at the quantum well barrier interface for thin MQWs. Meanwhile, the pronounced red shift in PL and an increase in the excitation lifetime in thicker MQWs is attributed to manifestation of the QCSE due to intrinsic field. Also, MWQs of larger thickness were shown to possess larger variations in potential profile and a larger amount of structural defects. The performed optical and microstructure analysis evidences an improvement of the MQW structural quality and increased emission efficiency in the thicker structures upon post-growth thermal annealing.

Acknowledgements

This research was partially supported by the joint Lithuanian–Latvian–Taiwan grant, by the European Commission supported SELITEC centre (Contract No. G5MA-CT-2002-04047), and by National Science Council, The Republic of China, under the grants NSC 90-2112-M-002-052, NSC 90-2215-E-002-027, and NSC 90-2215-E-002-041.

References

[1] S. Nakamura and G. Fasol, *The Blue Laser Diode: GaN Based Light Emitters and Lasers* (Springer, Berlin, 1997).

[2] A. Žukauskas, M.S. Shur, and R. Gaska, *Introduction to Solid-State Lighting* (Wiley, New York, 2002).

[3] J.-S. Tsang, J.-D. Guo, S.-H. Chan, M.-S. Feng, and C.-Y. Chang, Jpn. J. Appl. Phys. **36**, 1728 (1997).

[4] L.T. Romano, M.D. McCluskey, C.G. Van de Walle, J.E. Northrup, D.P. Bour, M. Kneissl, T. Suski, and J. Jun, Appl. Phys. Lett. **75**, 3950 (1999).

[5] C.-C. Chou, C.-M. Lee, and J.-I. Chyi, Appl. Phys. Lett. **78**, 314 (2001).

[6] R. Singh, D. Doppalapudi, T.D. Moustakas, and L.T. Romano, Appl. Phys. Lett. **70**, 1089 (1997).

[7] M.D. McCluskey, L.T. Romano, B.S. Krusor, D.P. Bour, N.M. Johnson, and S. Brennan, Appl. Phys. Lett. **72**, 1730 (1998).
[8] D. Doppalapudi, S.N. Basu, K.F.Jr. Ludvig, and T.D. Moustakas, J. Appl. Phys. **84**, 1389 (1998).
[9] Y.-T. Moon, D.-J. Kim, K.-M. Song, C.-J. Coi, S.-H. Han, T.-Y. Seong, and S.-J. Park, J. Appl. Plys. **89**, 6514 (2001).
[10] I.H. Ho and G.B. Stringfellow, Appl. Phys. Lett. **69**, 2701 (1996).
[11] S.Yu. Karpov, J. Nitride Semicond. Res. **3**, 16 (1998).
[12] K. Osamura, K. Nakajima, and Y. Murakami, Solid State Commun. **11**, 617 (1972).
[13] Y.-S. Lin, K.-J. Ma, C. Hsu, Y.-Y. Chung, C.-W. Liu, S.-W. Feng, Y.-C. Cheng, M.-H. Mao, C.C. Yang, H.-W. Chuang, C.-T. Kuo, J.-S. Tsang, and T.E. Weirich, Appl. Phys. Lett. **80**, 2571 (2002).
[14] S.-W. Feng, Y.-Y. Chung, C.-W. Liu, Y.-C. Cheng, C.C. Yang, M.-H. Mao, Y.-S. Lin, K.- J. Ma, and J.-I. Chyi, Appl. Phys. Lett. **80**, 4375 (2002).
[15] S. Chichibu, T. Azuhata, T. Sota, and S. Nakamura, Appl. Phys. Lett. **70**, 2822 (1997).
[16] S. Chichibu, T. Sota, K. Wada, and S. Nakamura, J. Vac. Sci. Technol. B **16**, 2204 (1998).
[17] K.P. O'Donnell, R.W. Martin, and P.G. Middleton, Phys. Rev. Lett. **82**, 237 (1999).
[18] Y.-H. Cho, T.J. Schmidt, S. Bidnyk, G.H. Gainer, J.J. Song, S. Keller, U.K. Mishra, and S.P. DenBaars, Phys. Rev. B **61**, 7571 (2000).
[19] P.R. Kent and A. Zunger, Appl. Phys. Lett. **79**, 1997 (2001).
[20] J.P. O'Neill, I.M. Ross, A.G. Cullis, T. Wang, and P.J. Parbrook, Appl. Phys. Lett. **83**, 1965 (2003).
[21] T.M. Smeeton, M.J. Kappers, J.S. Barnard, M.E. Vickers, and C.J. Humphreys, Appl. Phys. Lett. **83**, 5419 (2003).
[22] Y. Narukawa, Y. Kawakami, S. Fujita, and S. Nakamura, Phys. Rev. B **59**, 10283 (1999).
[23] S.D. Baranovskii, R. Eichmann, and P. Thomas, Phys. Rev. B **58**, 13081 (1998).
[24] K. Kazlauskas, G. Tamulaitis, A. Zukauskas, M.A. Khan, J.W. Yang, J. Zhang, G. Simin, M.S. Shur, and R. Gaska, Appl. Phys. Lett. **83**, 3722 (2003).
[25] M.S. Minsky, S. Watanabe, and N. Yamada, J. Appl. Phys. **91**, 5176 (2002).
[26] F. Bernardini and V. Fiorentini, Phys. Rev. B **58**, 15292 (1998).
[27] P. Lefebvre, A. Morel, M. Gallart, T. Taliercio, J. Allègre, B. Gil, H. Mathieu, B. Damilano, N. Grandjean, and J. Massies, Appl. Phys. Lett. **78**, 1252 (2001).
[28] W.W. Chow, H. Amano, T. Takeuchi, and J. Han, Appl. Phys. Lett. **75**, 244 (1999).
[29] T. Böttcher, S. Einfeldt, V. Kirchner, S. Figge, H. Heinke, D. Hommel, H. Selke, and P.L. Ryder, Appl. Phys. Lett. **73**, 3232 (1998).
[30] M. Shimizu, Y. Kwaguchi, K. Hiramatsu, and N. Sawaki, Solid-State Electron. **41**, 145 (1997).

ATKAITINIMO ĮTAKA InGaN / GaN DAUGIALAKŠČIŲ DARINIŲ OPTINĖMS SAVYBĖMS

Y.-C. Cheng [a], S.-W. Feng [a], C.C. Yang [a], C.-T. Kuo [b], J.-S. Tsang [b], S. Juršėnas [c], S. Miasojedovas [c], A. Žukauskas [c]

[a] *Nacionalinis Taivanio universitetas 1, Taipėjus, Taivanis*
[b] *Chsinčiu pramonės parkas, Chsinčiu, Taivanis*
[c] *Vilniaus universitetas, Vilnius, Lietuva*

Santrauka

Ištirtos ką tik išaugintų ir 30 min 800 °C temperatūroje atkaitintų $In_{0,15}Ga_{0,85}N$ / GaN daugialakščių darinių liuminescencijos, sužadinimo spektrų bei laike išskleistos liuminescencijos 10–300 K temperatūroje savybės, kurios palygintos su didelės skyros elektronų mikroskopijos atvaizdais. Pastebėta, kad kvantinių darinių atkaitinimas lemia optinių savybių pakitimą, kuris sudėtingai priklauso nuo kvantinės duobės storio. Plonose kvantinėse duobėse pastebėtas liuminescencijos smailės poslinkis į didesnės energijos sritis bei būdingi pakitimai sugerties spektre, dėl indžio difuzijos į barjerinę sritį. Platesnėse (3 nm) duobėse pastebėtas liuminescencijos smailės poslinkis į mažesnės energijos sritis bei išaugusi krūvininkų gyvavimo trukmė. Taip atsitinka, elektronų bei skylių banginėms funkcijoms atsiskyrus erdvėje dėl sumažėjusių potencialo fliuktuacijų. Plačiausiose (4 nm) kvantinėse duobėse atkaitinimas padarė dar didesnę įtaką sandarai, žymiai sumažindamas krūvininkų lokalizacijos energiją (poslinkis į didesnės energijos sritis didesnis nei vidinio elektrinio lauko nulemtas poslinkis į mažesnės energijos sritis) bei sumažino nespindulinę rekombinaciją (suintensyvėjo liuminescencija). Aiškinama, kad tokie rezultatai gauti dėl atkaitinimo sukeltos In–Ga abipusės difuzijos, kai priklausomai nuo duobės storio arba indis difunduoja į barjerinę sritį, arba vyksta indžio kondensacija (neigiama difuzija) pačiose kvantinėse duobėse.